Numerical Model of Total Artificial Heart Hemodynamics and the Effect of Its Size on Stress Accumulation

Gil Marom, Wei-Che Chiu, Marvin J. Slepian and Danny Bluestein

Abstract— **The total artificial heart (TAH) is a bi-ventricular mechanical circulatory support device that replaces the heart in patients with end-stage congestive heart failure. The device acts as blood pump via pneumatic activation of diaphragms altering the volume of the ventricular chambers. Flow in and out of the ventricles is controlled by mechanical heart valves. The aim of this study is to evaluate the flow regime in the TAH and to estimate the thrombogenic potential during systole. Toward that goal, three numerical models of TAHs of differing sizes, that include the deforming diaphragm and the blood flow from the left chamber to the aorta, are introduced. A multiphase model with injection of platelet particles is employed to calculate their trajectories. The shear stress accumulation in the three models are calculated along the platelets trajectories and their probability density functions, which represent the 'thrombogenic footprint' of the device are compared. The calculated flow regime successfully captures the mitral regurgitation and the flows that open and close the aortic valve during systole. Physiological velocity magnitudes are found in all three models, with higher velocities and increased stress accumulation predicted for smaller devices.**

I. Introduction

Though heart transplantation is the ideal treatment for patients with end-stage congestive heart failure (CHF), the shortage of donor organs requires a viable solution. The SynCardia total artificial heart (TAH; SynCardia Systems, Tucson, AZ) is a complete bi-ventricular cardiac replacement system useful for bi-ventricular failure [1]. Since 2004 the TAH has been approved for use by the Food and Drug Administration (FDA) in the United States as a bridge-to-transplant device for patients at imminent risk of death from bi-ventricular heart failure [2]. The original TAH has a maximum stroke volume of 70 cc. However, smaller adults and pediatric patients are often unable to receive this TAH due to anatomical constraints [3]. In order to accommodate these patients, a smaller 50 cc TAH considered for smaller patients and possible pediatric use has been designed [4].

This study was funded by grants from the National Institute of Health: NIBIB Quantum Award: Implementation Phase II - U01 EB012487-0 (D.B.).

G. Marom, W.C. Chiu, M.J. Slepian and D. Bluestein are with the Department of Biomedical Engineering, Stony Brook, NY 11794 USA (e-mail: gil.marom@stonybrook.edu).

M.J. Slepian is also with the Departments of Medicine and Biomedical Engineering, Sarver Heart Center, University of Arizona, Tucson, AZ 85724 USA.

Both the 70 cc and 50 cc TAHs are bi-ventricular replacement devices with similar design. Each chamber pumps blood via pneumatic displacement of a polymer diaphragm [5]. Since the TAH emulates the pulsatile blood flow of native hearts, valves are required for regulating and directing the flow into and out of the chambers. These mechanical Medtronic Hall heart valves (Medtronic Inc., Minneapolis, MN) are installed at the inlet and outlet of each chamber [5]. Similar to most currently available Mechanical circulatory support (MCS) devices, TAHs cause non-physiologic flow patterns and high flow shear stresses [6, 7]. While these elevated stresses may lead to platelet activation [8], to date the TAH has had a clinically acceptable thrombosis rate, being significantly lower than that observed with bi-ventricular assist devices (Bi-VADs) [9, 10].

Numerical methods can be employed to calculate the shear stress field, as well as other hemodynamics aspects, and provide detailed insights that experiments cannot capture. Computational Fluid Dynamics (CFD) and Fluid Structure Interaction (FSI) models were previously used in simulations of various mechanical valves [11-14] and MCS devices [15, 16]. Sonntag et al. [17] employed FSI model to simulate the flow in the ReinHeart TAH device, where the diaphragm motion is controlled by a piston rather than air pump. Still, this study neglected the valves by imposing a simple open or closed boundary conditions.

Although the influence of mechanical heart valves and MCS devices on platelet activation is well known, no previous study has investigated their influence on the hemodynamics in the Syncardia TAH using numerical models. The aim of the current study was to evaluate the flow regime in the 50 cc TAH and to estimate the risk of platelet damage relative to larger and smaller TAH ventricles. Toward that goal, a numerical model of the TAH, that includes the deforming diaphragm and the blood flow from the left chamber to the aorta, was introduced. A multiphase model with injection of platelet particles is employed to calculate their trajectories and stress accumulation distribution. These results are compared with two additional models of larger and smaller TAHs.

II. Methods

The present models focus on the flow in the left chamber of TAH. The geometry of 50 cc TAH was reconstructed from the original TAH design with Medtronic Hall mechanical valves in the mitral and aortic positions. The valves were oriented with 55° between them based on optimization for reduced thrombogenicity. During systolic phase the valvular motions are relatively limited, thus, as a first step toward full

978-1-4244-7929-0/14/$26.00 ©2014 IEEE

FSI model, the mitral and aortic valves were positioned in their fully closed and fully open configurations, respectively, (Fig. 1). The diaphragm was modeled to move from peak systolic to diastolic position by a contact with a pushing ball, using the finite element ANSYS Mechanical package (ANSYS Inc., Canonsburg, PA). A new fluid domain was generated based on the calculated diastolic position, representing the geometry of the left ventricle chamber with extended straight tubes that were connected to the two valves. Tetrahedral mesh with 5.4 million cells was generated for the flow domain. This mesh includes boundary layer cells in the vicinity of the diaphragm and mesh refinement near the valves. Larger and smaller models, with length scaling of 1.1 and 0.91, or maximum stroke volumes of 66.6 and 37.7 cc, respectively, are also modeled for comparison of flow stress levels. These dimensions were chosen to comply with available valves with diameters between 16 to 22 mm.

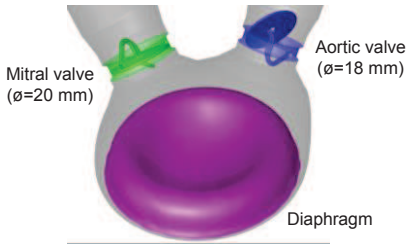

Figure 1. Valvular systolic configuration and the calculated initial position of the diaphragm in the FSI model of the 50cc Syncardia TAH.

The position of the diaphragm at every time step is represented by radial biquadratic function. The polynomial coefficients at the peak systolic and diastolic positions are based on the designed and calculated positions, respectively, as shown in Fig. 2. The motion of the diaphragm is calculated by assuming the polynomial coefficients has a sinusoidal function over time. The frequency of the function is based on the heart rate of each device, namely 120, 140 and 164 bpm for the 66.6, 50 and 37.7 cc TAHs, respectively. This motion of the diaphragm is modeled with user defined functions, while the motion of the fluid mesh is calculated by diffusion and remeshing algorithms. Representative cross sections of the mesh at the beginning, during, and at the end of systole are presented in the first row of Fig. 3. As a first step toward employing physiological one-dimensional flow boundary conditions, the outlet of the tube in the aortic side is defined as a zero pressure, and the closed mitral valve is represented with a closed tube.

Platelet trajectories are calculated by employing multiphase model with particles injection. Approximately 20 thousand spherical particles, with constant diameter of 3 μm and the density of the surrounding fluid, are released from a surface within the chamber. The stress history of these platelet particles are collected and rendered to calculate the stress accumulations for each platelet trajectory. The stress accumulation is defined herein as the linear product of the stress magnitude and the exposure time [12]. In order to efficiently represent the stress accumulation of thousands of trajectories, Probability Density Function (PDF) method is employed to statistically represent the stress accumulation distribution, or the thrombogenic footprint of the device [12]. The three TAHs are compared by the median values of stress accumulation and their distribution.

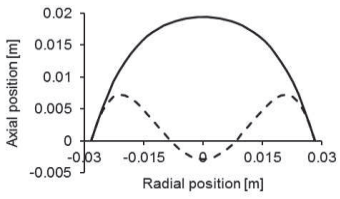

Figure 2. The radial position of the diaphragm during peak systole (continuous line) and diastole (dashed line).

The model is solved by ANSYS Fluent (ANSYS Inc., Canonsburg, PA) assuming the blood is Newtonian and isothermal at temperature of 37°C. As a first step toward modeling the laminar-turbulent transition, the flow was assumed to be laminar as in previous models of rigid mechanical valve [18]. To improve the convergence of the dynamic mesh model the blood is modeled as a compressible liquid [19]. A finite volume method was employed for solving the unsteady 3D Navier-Stokes and mass conservation equations using Arbitrary Lagrangian Eulerian (ALE) approach for the dynamic mesh. The implicit flow solver uses second order spatial scheme and temporal discretization.

III. Results

Comparison of the results of the three models is presented in this section. First, detailed results of the 50 cc model are described, including the flow velocity field and the particles trajectories. Then, the PDF distributions of the three models are compared.

A. Base case: Syncardia 50 cc TAH

The second row of Fig. 3 shows the velocity vectors at three different times during systole. At the beginning of systole (t=25 ms) a strong flow through the aortic valve is found. This strong aortic flow, with maximum velocity of 1.8 m/s inside the center hole of the disk, opens the aortic valve after the diastole. A regurgitant flow through the mitral valve is found with velocity magnitude of 0.6 m/s. This regurgitant flow was stronger earlier in the cardiac cycle. Fig. 4 presents a zoom on the mitral valve at t=10 ms. At this time the blood flow through the central hole of the mitral disc reaches velocity of 1.4 m/s. This jet creates a vortex ring that decays rather quickly and can hardly be noticed at t=25 ms. Another interesting flow patterns are found on the chamber side of the mitral valve at both times (10 and 25 ms, Figs. 4 and 3, respectively). These vortices are a caused by the back step effect of the smaller tube near the closed valve. Later at systole, when the diaphragm reaches its fully inflated position (t=210 ms), the velocity of the flow through the aortic valve decreased to 0.5 m/s as a results of the diaphragm deceleration before starting the reverse motion. The direction of this flow is controlled mainly by the opening angle of the valve. At the end systole (t=400 ms), the strong backflow in the aortic valve should close this valve before reaching the diastole, but since the valves here are still assumed stationary this motion cannot be captured here. It is also worth noting that although the duration of the mitral

regurgitation is very short, low velocity flow field is found leeward of the mitral valve until the end of systole.

The particle locations at the three times are shown in the third row of Fig. 3. The particles are colored by the local laminar stress magnitude that is calculated based on the surrounding fluid. The location of the particle releasing surface can be seen at the beginning of systole (t=25 ms), since the particles movement is still relatively small at this time. As expected, the locations with the highest stress magnitudes are always near the aortic valve and the moving diaphragm. The fact that almost none of the particles seems to flow through the mitral valve indicates that although the regurgitating flow could be quite fast, its mass flow is almost negligible. It is also interesting that the back and forth motion of the diaphragm disperse the particles in the chamber almost evenly until the end of systole.

B. Comparison with 66.6 and 37.7 cc devices

In order to compare the velocity magnitudes of the three models, a relative time that represent the systolic flow to the aorta need to be defined. A relative time of 30% of the cardiac cycle is chosen here since it is before the deceleration and the flow velocities are still relatively large. At this relative time, the maximum velocity magnitudes increase with the decrease of the device's dimensions (1.24, 1.16 and 0.98 m/s for the 37.7, 50 and 66.6 cc TAHs, respectively). The stress accumulation distribution of the three models are represented by their PDFs in Fig. 5. It should be noted that the horizontal logarithmic axis is divided into stress accumulation lower and higher than 10 dyne·s/cm^2. As might be expected, there is an increasing probability that platelets in smaller devices will be subjected to higher stress accumulation values. This could be attributed to both the reduced size and by the higher pumping frequencies, or heart rates, that accelerate the blood flow. It can also be demonstrated from the median stress accumulations of 3.41, 2.19 and 1.12 dyne·s/cm^2, for the 37.7, 50 and 66.6 cc TAHs, respectively (marked as vertical dashed lines in Fig. 5). The probability for stress accumulation of more than 10 dyne·s/cm^2 is lower than 1% for all the three models. While this probability might be considered negligible, the trend of higher probability for elevated stresses in smaller TAHs is kept. Although these findings might indicate that platelets in smaller TAHs are more prone to damage, it should be noted that large part of the histograms are overlapping. Therefore, it is reasonable to assume that their thrombogenic potential is very similar. However, smaller TAHs could be further improved by a dedicated design instead of the simple scaling down that is presented here.

IV. CONCLUSIONS

Numerical models of the TAH of three differing sizes with deforming diaphragm and particles injection, have been

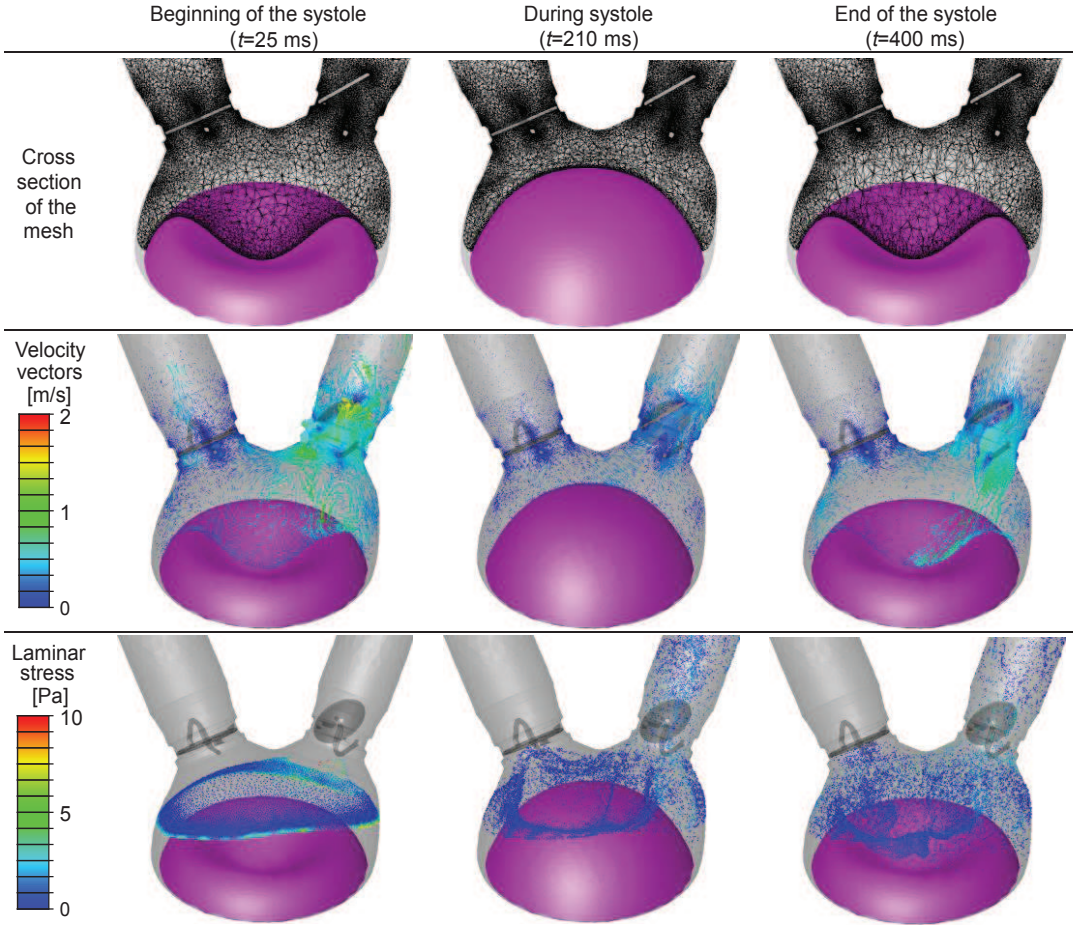

Figure 3. The 50 cc Syncardia TAH model at three times during systole. Representative cross sections of the mesh and velocity vectors are shown in the first and second rows, respectively. Particles location and their local laminar stress values are shown in the third row.

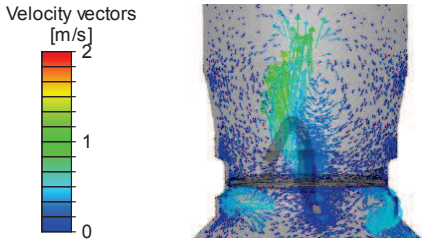

Figure 4. Zoom in on the mitral regurgitation at the beginning of systole (t=10 ms).

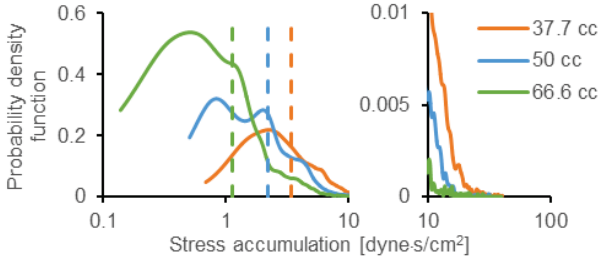

Figure 5. Probability Density Function (PDF) of the stress accumulation of the three TAHs with different sizes. The vertical dashed lines mark the median values. The horizontal logarithmic axis is divided into stress accumulation lower and higher than 10 dyne·s/cm^2.

developed. These models focused on the systolic phase, and the valves were positioned accordingly. The resulting flow regime captured the mitral regurgitation and the strong flows that open and close the aortic valve. There is a mild trend of increased probability that platelets in smaller devices will be exposed to elevated stresses because of the combined effect of higher pumping frequency and smaller dimensions that may translate into a mild increase in platelet activation. Utilizing our device thrombogenicity emulation (DTE) methodology that we have previously employed for optimizing the thromboresistance of mechanical circulatory support devices, minor design changes may mitigate this potential increase in shear activation [6]. Necessarily the ultimate thrombogenicity determination will require clinical observation and in human assessment.

ACKNOWLEDGMENT

We thank Matthew Pollack from Boston University for his help in reconstructing the geometry. We also thank Doug Nutter and Richard Smith for information on TAH engineering drawings and operating conditions. The software provided by ANSYS Academic Partnership with Stony Brook University.

REFERENCES

[1] J. G. Copeland, R. G. Smith, F. A. Arabia, P. E. Nolan, G. K. Sethi, P. H. Tsau, et al., "Cardiac replacement with a total artificial heart as a bridge to transplantation," New England Journal of Medicine, vol. 351, pp. 859-867, Aug 26 2004.

[2] M. J. Slepian, R. G. Smith, and J. C. Copeland, "The SynCardia CardioWest Total Artificial Heart," in Treatment of Advanced Heart Disease. vol. 56, K. L. Baughman and W. A. Baumgartner, Eds., ed New York, NY: Taylor & Francis Group, 2006, pp. 473 – 490.

[3] O. H. Frazier and W. E. Cohn, "Continuous-flow total heart replacement device implanted in a 55-year-old man with end-stage heart failure and severe amyloidosis," Tex Heart Inst J, vol. 39, pp. 542-6, 2012.

[4] M. J. Slepian, Y. Alemu, G. Girdhar, J. S. Soares, R. G. Smith, S. Einav, et al., "The Syncardia total artificial heart: in vivo, in vitro, and computational modeling studies," J. Biomech., vol. 46, pp. 266–275, 2013.

[5] A. Platis and D. F. Larson, "CardioWest temporary total artificial heart," Perfusion, vol. 24, pp. 341-346, Sep 2009.

[6] G. Girdhar, M. Xenos, Y. Alemu, W. C. Chiu, B. E. Lynch, J. Jesty, et al., "Device thrombogenicity emulation: a novel method for optimizing mechanical circulatory support device thromboresistance," PLoS One, vol. 7, p. e32463, 2012.

[7] M. Xenos, G. Girdhar, Y. Alemu, J. Jesty, M. Slepian, S. Einav, et al., "Device Thrombogenicity Emulator (DTE)-design optimization methodology for cardiovascular devices: a study in two bileaflet MHV designs," J Biomech, vol. 43, pp. 2400-9, Aug 26 2010.

[8] M. H. Kroll, J. D. Hellums, L. V. McIntire, A. I. Schafer, and J. L. Moake, "Platelets and shear stress," Blood, vol. 88, pp. 1525-41, Sep 1 1996.

[9] B. G. Leshnower, R. G. Smith, M. L. Ohara, J. Woo, A. Pochettino, R. J. Morris, et al., "Is the total artificial heart superior to BIVAD therapy as a method of bridging patients to heart transplantation?," presented at the 43rd Annual meeting of the Society of Thoracic Surgeons, San Diego, CA, 2007.

[10] J. G. Copeland, H. Copeland, M. Gustafson, N. Mineburg, D. Covington, R. G. Smith, et al., "Experience with more than 100 total artificial heart implants," J Thorac Cardiovasc Surg, vol. 143, pp. 727-34, Mar 2012.

[11] K. E. Richards, D. Deserranno, E. Donal, N. L. Greenberg, J. D. Thomas, and M. J. Garcia, "Influence of structural geometry on the severity of bicuspid aortic stenosis," Am. J. Physiol. Heart Circ. Physiol., vol. 287, pp. H1410-H1416, 2004.

[12] Y. Alemu and D. Bluestein, "Flow-induced platelet activation and damage accumulation in a mechanical heart valve: numerical studies," Artif Organs, vol. 31, pp. 677-88, Sep 2007.

[13] I. Borazjani, G. Iman, and F. Sotiropoulos, "High-resolution fluid-structure interaction simulations of flow through a bi-leaflet mechanical heart valve in an anatomic aorta," Ann. Biomed. Eng., vol. 38, pp. 326-344, 2010.

[14] T. Hong and C. N. Kim, "A numerical analysis of the blood flow around the bileaflet mechanical heart valves with different rotational implantation angles," J. Hydrodyn. Ser. B, vol. 23, pp. 607-614, 2011.

[15] W. C. Chiu, M. J. Slepian, and D. Bluestein, "Thrombus formation patterns in the HeartMate II VAD- clinical observations can be predicted by numerical simulations," ASAIO J, Jan 24 2014.

[16] J. Zhang, P. Zhang, K. H. Fraser, B. P. Griffith, and Z. J. Wu, "Comparison and experimental validation of fluid dynamic numerical models for a clinical ventricular assist device," Artif Organs, vol. 37, pp. 380-9, Apr 2013.

[17] S. J. Sonntag, T. A. S. Kaufmann, M. R. Busen, M. Laumen, T. Linde, T. Schmitz-Rode, et al., "Simulation of a pulsatile total artificial heart: Development of a partitioned Fluid Structure Interaction model," Journal of Fluids and Structures, vol. 38, pp. 187-204, Apr 2013.

[18] A. P. Yoganathan, K. B. Chandran, and F. Sotiropoulos, "Flow in prosthetic heart valves: state-of-the-art and future directions," Ann Biomed Eng, vol. 33, pp. 1689-94, Dec 2005.

[19] G. Marom, R. Haj-Ali, E. Raanani, H. J. Schafers, and M. Rosenfeld, "A fluid-structure interaction model of the aortic valve with coaptation and compliant aortic root," Med Biol Eng Comput, vol. 50, pp. 173-82, Feb 2012.